Systematic Chemical Effects Observed in "Atomic" X-ray Absorption Fine Structure

W. E. O'Grady,*,† X. Qian,‡ and D. E. Ramaker†,‡

Code 6170, Chemistry Division, Naval Research Laboratory, Washington, D.C. 20375, and Chemistry Department, George Washington University, Washington, D.C. 20052

Received: March 18, 1997; In Final Form: May 29, 1997[⊗]

We report here, for the first time, large and systematic chemical effects on the "atomic" X-ray absorption fine structure (AXAFS) for a series of Pt−Ru alloys as a function of the composition and for an *in situ* Pt electrode as the electrode potential is increased. These changes are seen in the Fourier transform of the normal $\chi(E)$ function in XAFS, where the AXAFS produces a peak at the characteristic atomic radius. Curved-wave multiple-scattering cluster calculations (FEFF6) confirm the changes with alloy composition and electrode potential, although the theory overestimates the size of the changes. Obvious reasons for this are given. The systematic chemical effects and agreement with theoretical predictions provide strong support for their interpretation as AXAFS features, rather than multielectronic excitations. The AXAFS structure and its interpretation offers the promise of providing a new tool for observing *in situ electronic* (AXAFS) and *geometric* (normal EXAFS) structural changes simultaneously in complex systems where long range order is not required.

Introduction

X-ray absorption fine structure (XAFS) provides an extraordinary technique for the *in situ* study of electrochemical interfaces[1] and catalysts,[2] primarily because the Fourier transform of this structure is known to reflect the radial distributions of other neighboring atoms about the absorber. However, peaks have often been observed at very short distances that could not be attributed to meaningful bond lengths. Recently Rehr et al.[3] attributed these peaks to "atomic" XAFS (AXAFS) scattering and suggested that they might serve as a probe of chemical effects. Holland et al.[4] showed many years ago that scattering of the photoejected electrons off of the interatomic potential associated with the absorber atom can produce oscillations in the "background" and first called these oscillations AXAFS.[4] We report here, for the first time, large and systematic chemical effects on this structure for a series of Pt−Ru alloys as a function of the composition and for an *in situ* Pt electrode as the electrode potential is increased. The AXAFS structure and its interpretation offers the promise of providing a new tool for observing *in situ electronic* (in the AXAFS) and *geometric* (in the normal EXAFS) structural changes simultaneously in complex systems where long range order is not required.

The peaks routinely observed in the low R range ($R < 1.5$ Å) of FT[$\chi(k)$] have often been disturbing and controversial because they could not be attributed to meaningful bond lengths. In spite of the recent physical interpretation sited above, the existence of such AXAFS is still controversial since the structure in the background that strongly affects the low-R-range peaks has been attributed for years to multielectron excitations.[5,6] The large and systematic chemical effects on the low R peaks found in this work and the agreement with theoretical AXAFS predictions are significant in this regard. Further, the presence of such structure for metals where multielectron effects are usually smaller than in the metal oxides that were the subject of previous AXAFS work[4] provides strong evidence for the appropriateness of the AXAFS interpretation in the systems studied here, and therefore for many other systems as well.

Experimental Section

Platinum ruthenium black alloys of varying composition were prepared by the formaldehyde reduction of the metal salts in a basic solution. Following the preparation, all of the samples were given a heat treatment at 900 °C in nitrogen to ensure alloy formation. X-ray diffraction showed all the samples to be alloys. The XAFS samples were prepared by thoroughly mixing each alloy sample with boron nitride (Aldrich Chemicals) and pressing them into self-supporting pellets that were mounted on an aluminum holder and placed into a styrofoam Dewar where the Pt L_3 edge XAFS data were collected at 77 K in the transmission mode.

For the *in situ* XAFS experiments on the Pt electrodes, Teflon-bonded electrodes were fabricated using Prototeck Co. 10 wt % Pt supported on carbon catalyst. The electrodes were made following the procedure described earlier.[7] For the XAFS measurements a cell similar to that described previously for the *in situ* nickel oxide electrode studies was used.[7] Nafion was used as the separator, and the Pt/C electrode was held in a PTFE gasket and was flooded with 0.1 M H_2SO_4. The counter electrode was a flooded uncatalyzed high surface area carbon electrode held in a PTFE gasket, and the reference electrode was a Pd/H electrode. The cell was placed in the beam, the potential was controlled with a PARC 273 potentiostat, and the Pt L_3 edge XAFS were collected at room temperature in the transmission mode.

XAS measurements were performed on beam line X-11A of the National Synchrotron Light Source (NSLS) at Brookhaven National Laboratory. The NSLS storage ring operated at 2.52 GeV beam energy with ring currents between 40 and 200 mA. The Si(111) double-crystal monochromator was detuned by 30% at the Pt L_3 edge (11564 eV) to minimize the presence of higher harmonics in the beam. The energy calibration was achieved by measuring the XAFS of a 7 μm thick Pt foil. The intensities of the incident (I_0) and transmitted (I) X-rays were measured with gas flow ion chambers and the gas compositions of the ion chambers adjusted such that the I_0 and I chambers absorbed 10% and 80% of the incoming X-rays, respectively.

Results and Discussion

Figure 1 shows a qualitative picture illustrating the atomic potentials involved on the absorber (A) and on a nearby scatterer

† Naval Research Laboratory.
‡ George Washington University.
⊗ Abstract published in *Advance ACS Abstracts,* July 1, 1997.

S1089-5647(97)00967-X CCC: $14.00

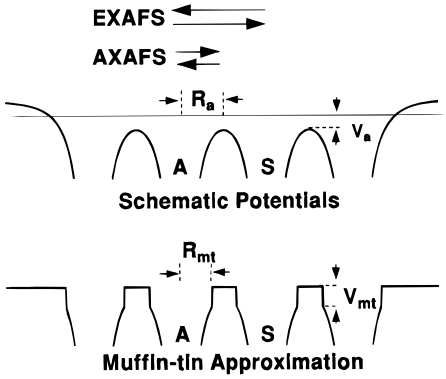

Figure 1. Illustration of schematic potentials in a solid showing the EXAFS and AXAFS scattering with the electron wave initiated at the absorber (A) and scattered by either the neighboring atom (S) or by the interatomic potential at the periphery of the absorber. The parameters R_a and V_a, characterizing the potential, are illustrated as shown. Also shown is the usual muffin-tin approximation such as that utilized in the FEFF6 code with R_{mt}, $V°_{mt}$, and V_{mt} defined as illustrated.

(S), not necessarily bonded to one another. From elementary quantum mechanics we know that electrons can scatter off of a potential; in this case either off of the potential near the core of a neighboring scattering atom (S) giving the normal EXAFS oscillations or off of the potential in the interatomic region giving the AXAFS oscillations. The potential is characterized by R_a, the effective radius of the atom, and V_a, the potential relative to the interstitial zero potential, as illustrated in Figure 1. These characteristics are mapped directly onto FT[$\chi(E)$], with a peak near the distance R_a and with the magnitude of the AXAFS peak directly proportional to $|V_a|$.

In XAS, the oscillatory nature of the EXAFS function $\chi(E) = [\mu(E) - \mu_0(E)]/\mu_0(E)$ contains the desired information. The analysis involves a background, $\mu_0(E)$, removal from the spectrum followed by a Fourier transform (FT) of $\chi(E)$ into R-space.[8] This background removal is done by a well-known spline-smoothing procedure, with specific criteria used to determine the desired level of smoothing for optimal background removal.[9] Although some new iterative background removal procedures have been reported recently,[10,11] which leave the AXAFS in the background, we use the standard analysis procedure here, except the criteria for the background removal is modified, since previously efforts were made to remove the features in FT[$\chi(E)$] at low R. This standard procedure places the AXAFS structure in χ which results in low R features in FT[$\chi(k)$]. Figure 2a shows FT[$k\chi(k)$] for three different smoothing levels on the Pt electrode data. These data clearly reveal the dramatic reductions with smoothing level for $R < 0.5$ Å and the relatively small changes exhibited in the primary Pt−Pt EXAFS feature around 2.2 Å and even in the AXAFS feature around 1.5 Å. Our criteria is to reduce the FT[$k^n\chi(k)$] as R goes to zero as much as possible, without removing any of the Pt−Pt EXAFS contribution, and to examine this in both the FT of $k^1\chi(k)$ and $k^3\chi(k)$. Note that the AXAFS feature here in FT[$k^1\chi(k)$] is nearly 50% of the primary Pt−Pt EXAFS feature and is relatively unchanged in intensity with different smoothing levels as long as the primary EXAFS feature is unchanged. Thus we believe that the intensities given for the AXAFS are accurate to within around ±5%, and the systematic trends with chemistry are real. Note, that the AXAFS feature is even larger in FT-[$k^0\chi(k)$]. and this is shown for the final results.

Figure 3 illustrates the effects of a direct change in chemical environment about the Pt atom in a series of Pt/Ru alloys. In this series the atoms and bond distances around the Pt atom change affecting the shape and height of the potential around the Pt atom and leading to modifications of the AXAFS

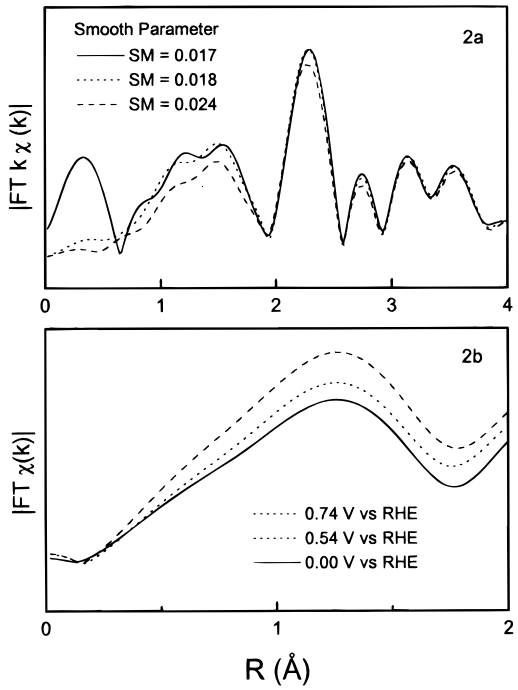

Figure 2. (a) Fourier transforms of $k^1\chi(k)$ ($0.5 < k < 8.5$) for Pt L_3 XAS data for the *in situ* Pt electrode showing three different smoothing parameters as defined by Sayers et al.[9] On the basis of our criteria, the dotted line gives the desired results for the optimal background subtraction. (b) Fourier transforms of $k^0\chi(k)$ ($0.5 < k < 8.5$) for Pt L_3 XAS data for the *in situ* Pt electrode at the indicated applied voltages relative to the reversible hydrogen electrode (RHE).

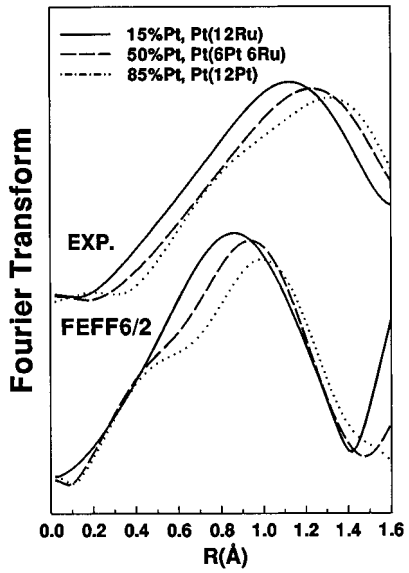

Figure 3. Fourier transforms of $k^0\chi(k)$ ($0.5 < k < 8.5$) for Pt L_3 XAS data taken in transmission at 77 K for Pt/Ru alloys with the relative compositions shown. Also shown are FEFF6 curved-wave cluster calculations on $PtRu_NPt_{12-N}$ clusters with $N = 0$, 6, and 12 and a Pt−Pt distance of 2.77 Å and Pt−Ru distances of 2.73 and 2.69 Å, respectively. The AXAFS contributions are superimposed on the normal EXAFS contributions, which begin around 1.5 Å.

observed. In Figure 3 the experimental results are compared with the results from curved-wave cluster calculations obtained with the FEFF6 code.[12] The results shown were obtained using clusters of the type $PtPt_{12-N}Ru_N$ ($N = 0$, 6, or 12).

The FEFF6 code makes the normal muffin-tin approximation to the potential, which is paramaterized by the muffin-tin radius, R_{mt}, and the potential height, V_{mt}, with R_{mt} generally smaller than R_a and $|V_{mt}|$ generally larger than $|V_a|$ as illustrated in Figure

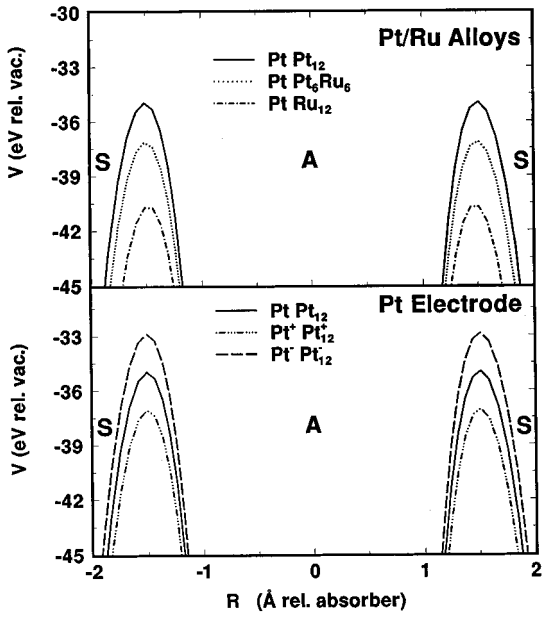

Figure 4. Comparison of the FEFF6 calculated potentials for different neighbors about a Pt absorber atom. Calculated results are shown for the three $PtPt_{12-N}Ru_N$ (N = 0, 6, 12) clusters utilized in Figure 2. Potentials are also shown for a $PtPt_{12}$ cluster where all of the Pt atoms were assumed to have either a positive or negative charge on them equal to that of 0.05 electrons by adding $\pm 0.05\ e^2/R$ to the potentials.

1. The calculations also included a 10% overlap of the muffin-tin spheres to provide better agreement with the experimental data because this overlap increases R_{mt} and decreases $|V_{mt}|$.[5] Still, the theory overestimates the AXAFS feature by a factor of 2 (note the FEFF6/2 in Figure 3). Although the muffin-tin approximation to the potential may not be entirely adequate for AXAFS, qualitative agreement is found for the peak positions and their changes as a function of the Pt−Ru alloy composition.

Figure 2b shows the data for the carbon-supported Pt electrode where the results clearly show a strong and systematic variation in peak height with changing applied electrode potential. Note that the peak positions do not change, consistent with a constant R_a or no change in the immediate chemical environment. The increasing intensities can be attributed to an increase in $|V_a|$ as the Pt electrode charge becomes more positive with increasing positive electrode potential.

In Figure 4 we qualitatively show the effects in the potential calculated with the FEFF6 code that give rise to the changes observed in the AXAFS. For the $PtPt_{12-N}Ru_N$ alloy case, as the average atomic radius becomes shorter with increase in n, the potential overlap increases leading to an increase in $|V_a|$, which increases the magnitude of the AXAFS scattering seen in Figure 3. For the Pt electrode case, a potential of the type $\pm 0.05\ e/R$ is superimposed on the previously unperturbed $PtPt_{12}$ potential to mimic the effects of the increase in electrode voltage in the positive direction. This leads to a strong narrowing of the potential and a subsequent increase in $|V_a|$ resulting in an increase in the AXAFS peak with increased voltage as shown in Figure 2b. Note that the calculation used 0.05 of an electron charge on each Pt atom, which corresponds to a charge of $\sim$30 $\mu C/cm^2$ estimated from the cyclic voltammetry reported by Clavilier et al.[13] for a spherical single-crystal Pt surface. Note also that for these 30 Å diameter Pt clusters, nearly 50% of the Pt atoms are surface atoms, so that the changes seen have the right order of magnitude for this system.

These results provide a new tool for observing changes in the interatomic potential simultaneously with the structural and electronic changes that produced them. Furthermore, this technique can be applied *in situ* to materials, such as catalysts, electrochemical systems, and alloys, which often cannot be studied by other means because of long range disorder, etc. Further quantitative studies of this effect are in progress.

Acknowledgment. Support for this work by the Office of Naval Research is gratefully acknowledged.

References and Notes

(1) Abruna, H. D. In *Electrochemical Interfaces: Modern Techniques for In Situ Interface Characterization*; Abruna, H. D., Ed.; VCH Publishers: New York, 1991; Chapter 1.

(2) Koningsberger D. C.; Prins, R. In *X-ray absorption:Principles, Applications and Techniques of EXAFS, SEXAFS and XANES*; Koningsberger, D. C., Prins, R., Eds.; John Wiley: New York, 1988; Chapter 8.

(3) Rehr, J. J.; Booth, C. H.; Bridges, F.; Zabinsky, S. I. *Phys. Rev. B*, **1994**, *49*, 12347.

(4) Holland, B. W.; Pendry, J. B.; Pettifer, R. F.; Bordas, J. *J. Phys. C* **1978**, *11*, 633.

(5) Filipponi, A.; Di Cicco, A. *Phys. Rev. B* **1996**, *53*, 9466.

(6) Rehr, J. J.; Booth, C. H.; Bridges, F.; Zabinsky, S. I. *Phys. Rev. B* **1996**, *53*, 9468.

(7) McBreen, J.; O'Grady, W. E.; Pandya, K. I.; Hoffman, R. W.; Sayers, D. E. *Langmuir*, **1987**, *3*, 428.

(8) Sayers, D. E.; Stern, E. A.; Lytle, F. W. *Phys. Rev. Lett.* **1971**, *27*, 1204.

(9) Cook, J. W.; Sayers, D. E., *J. Appl. Phys.* **1981**, *52*, 5024.

(10) Li, G. G.; Bridges, F.; Brown, G. S. *Phys. Rev. Lett.* **1992**, *68*, 1609.

(11) Bridges, F.; Booth, C. H.; Li, G. G. *Physica* **1995**, *B208/209*, 121.

(12) Zabinsky, S. I.; Rehr, J. J.; Ankudinov, A.; Albers, R. C.; Eller, M. *J. Phys. Rev. B* **1996**, *52*, 2995.

(13) Clavilier, J.; Armand, D. *J. Electroanal. Chem.* **1986**, *199*, 187.